Available online at www.sciencedirect.com
SCIENCE DIRECT®
Journal of Magnetic Resonance 161 (2003) 252–257
JMR Journal of Magnetic Resonance
www.elsevier.com/locate/jmr

Communication

NMR-microscopy with TrueFISP at 11.75 T

Sascha Köhler,* Karl-Heinz Hiller, Mark Griswold, Wolfgang R. Bauer, Axel Haase, and Peter M. Jakob

Physikalisches Institut, EP5, Universität Würzburg, Am Hubland, Würzburg 97074, Germany

Received 30 August 2002; revised 2 December 2002

Abstract

The purpose of this paper is to demonstrate that a fully balanced gradient echo technique (TrueFISP) can be used for microscopic experiments at high static magnetic field strengths. TrueFISP experiments were successfully performed on homogeneous and inhomogeneous objects at 11.75 T. High-resolution TrueFISP images were obtained from phantoms, plants, formalin-fixed samples, and from an isolated beating rat heart with an in-plane resolution of 78 μm and a slice thickness of 500 μm. The signal-to-noise ratio (SNR) gain of TrueFISP compared to conventional gradient echo or spin echo sequences will allow faster acquisition times or an improvement in spatial resolution for microscopic experiments.

Keywords: MRI; Fast imaging; Steady-state free precession; TrueFISP; High field; Microscopy

1. Introduction

The purpose of NMR microscopy is to look inside small structures. To this end, high spatial resolution and a satisfactory SNR are required in an acceptable imaging time. To fulfill these demands, microscopic experiments are normally performed at very high static field strengths. Imaging techniques with high SNR efficiency could improve spatial resolution or reduce drastically the imaging time in microscopic experiments, since the resolution in microscopic experiments is often limited by the achievable SNR.

Refocused steady-state sequences have recently gained popularity in clinical magnetic resonance imaging. The success of TrueFISP [1] (fast imaging with steady-state precession) in various applications is attributed to its high signal at short repetition times [2–5]. Because all gradients are refocused over a repetition interval and no RF spoiling is implemented, the transverse magnetization is maintained between successive RF pulses. Coherent transverse magnetization continues to contribute to the signal in successive repetition intervals, which results in a much higher SNR than in magnetization-spoiled imaging techniques [6]. The image contrast of TrueFISP is approximately proportional to $1/2(M_0(\mathrm{T2}/\mathrm{T1})^{1/2})$ [7,8]. However, TrueFISP is very sensitive to susceptibility differences and suffers from bands of signal loss in images due to B_0 inhomogeneity [9,10]. This off-resonance dependence of the steady-state TrueFISP magnetization is shown in Fig. 1. For alternating $\pm\alpha$ excitation pulses in successive repetition periods, the intensity profile shows a narrow signal drop if the phase offset (ϕ) due to off-resonance between successive RF pulses is $\pm\pi$. The period of this pattern is given by 1/TR. These banding artifacts can be avoided if the range of resonant frequencies across the image plane is within the plateau of this intensity profile. To achieve these requirements, a optimized shimming procedure and a very short TR are needed. The variation of frequencies should therefore be in the range of $\pm 1/(4\mathrm{TR})$, which corresponds to a field homogeneity of 62.5 Hz across the image plane for a TR of 4.0 ms.

However, this off-resonance behavior of TrueFISP is not only a drawback. It could rather be exploited as a novel tissue contrast mechanism. With an appropriate choice of sequence repetition time, all spins within a certain band of resonance frequencies can be suppressed while all other spins yield high signal. Moreover, the

* Corresponding author. Fax: +49-931/888-5851.
E-mail address: sakoehler@physik.uni-wuerzburg.de (S. Köhler).

1090-7807/03/$ - see front matter © 2003 Elsevier Science (USA). All rights reserved.
doi:10.1016/S1090-7807(03)00013-2

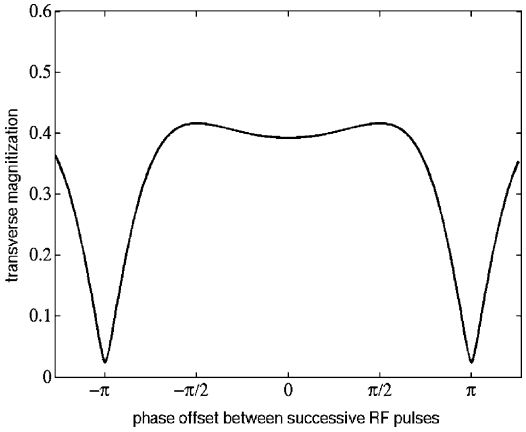

Fig. 1. Numerical calculation of steady-state transverse magnetization of TrueFISP as a function of the phase offset (ϕ) between successive RF pulses. The flip angle was 60°, T1 = 150 ms, T2 = 100 ms, and TR = 4 ms. The transverse magnetization shows strong signal drops at phase offsets $\pm\pi$, which are responsible for banding artifacts. The behavior of the transverse magnetization is periodic in frequency with a period of 1/TR. If the range of frequencies across the image plane is within the plateau of the intensity profile of the transverse magnetization, banding artifacts are avoided.

spectral profile of the sequence can be modified with different phase cycles of the radiofrequency pulse [11,12].

If the banding artifact could not be avoided due to shimming, it can be eliminated by acquiring two images: one with alternating RF phases and one with the same RF phase, which will shift the signal profile (Fig. 1) by half a period. By taking the maximum signal between the two images, an unartifacted image of essentially uniform intensity for certain tissues can be obtained [13].

Until recently, refocused steady-state sequences have been impractical for imaging applications due to the sensitivity to off-resonance effects. Especially at high fields, it has been difficult to achieve the postulated requirement on field homogeneity [14]. The purpose of the present study is to demonstrate that TrueFISP can in fact be used at high static magnetic field strengths for microscopic imaging experiments with faster acquisition times as compared to conventional gradient echo or spin echo experiments.

2. Methods

All experiments were performed on a Bruker AMX-500 microscopy system at 11.75 T with a maximum gradient strength of 660 mT/m. Transmission and reception of MR signal was achieved using a quadrature birdcage resonator (RAPID Biomedical, Germany) tuned to the ^{1}H frequency of 500.15 MHz. Both 2D and 3D TrueFISP sequences were implemented. As described by Deimling and Heid [15], each TrueFISP train was prepared by an $\alpha/2$ excitation pulse to bring magnetization close to the steady state and to minimize the oscillation of echo amplitudes after the start of excitation. A flip angle of 60° was adjusted for all TrueFISP experiments. A TR/TE = 2.7/1.35 ms was achieved with a matrix of 128 × 128. To obtain high-resolution images a matrix of 256 × 256 was used with a TR/TE = 4.0/2.0 ms. With a FOV of 20 × 20 mm a maximum spatial resolution of 78 μm in-plane was achieved. Experiments were performed on a water phantom doped with different concentrations of Gd-DTPA (1.0, 0.5, 0.25 mM, and water). To demonstrate the range of applications of TrueFISP at high fields, plants (sunflower), and formalin-fixed samples were also investigated. Finally, high-resolution segmented TrueFISP images [16] of a beating isolated rat heart were obtained. Hearts of male Wistar rats were excised and perfused in the Langendorff mode with Krebs–Henseleit buffer. Left ventricular pressure was measured using a balloon inserted in the left ventricle and connected to a pressure transducer. The pressure curve was registered by a personal computer, which performs trigger pulses to synchronize the MR pulse sequence to the heart cycle. Left ventricular end-diastolic pressure was adjusted to 5 mm Hg by the balloon volume. All experiments with animals were in accordance with the European regulation on care and use of laboratory animals.

Linewidths less than 45 Hz were obtained for all experiments. The TrueFISP images were compared to gradient echo and spin echo images of the same spatial resolution in terms of SNR and efficiency. The SNR was determined from the images by dividing the mean pixel value over the region of interest (ROI) by the standard deviation of the noise [17]. The SNR efficiency (η) is defined here as SNR per square root of total acquisition time.

3. Results

Fig. 2 shows a comparison between a TrueFISP and a FLASH image of a water phantom doped with different concentrations of Gd-DTPA. With a matrix of 256 × 256, an in-plane resolution of 78 μm was obtained with a slice thickness of 500 μm. On our system, we could achieve a TR/TE = 4.0/2.0 ms with the TrueFISP sequence and a TR/TE = 4.5/2.0 ms with the FLASH sequence. The longer TR in the FLASH sequence results from the need for sufficient spoiler gradients. This resulted in a total acquisition time of 16.4 s for the TrueFISP experiment and 18.4 s for the FLASH experiment. The SNR efficiency of the TrueFISP and FLASH experiment was calculated for three tubes filled with different Gd-DTPA concentrations and for the surrounding water (Table 1). An increase of Gd-DTPA concentration results in a reduction of T1 and thus leads to an enhancement of the SNR efficiency of the FLASH sequence in comparison to the

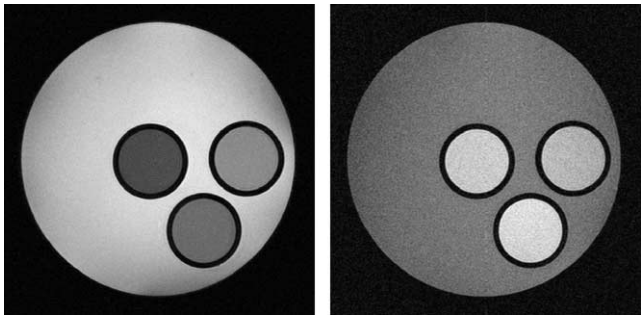

Fig. 2. Comparison between a TrueFISP (left) and a FLASH image (right) of a water phantom with an in-plane resolution of 78 μm and a slice thickness of 500 μm. The phantom is filled with 3 tubes doped with different concentrations of Gd-DTPA (1.0, 0.5, 0.25 mM, and water). Total acquisition time was 16.4 s for the TrueFISP experiment (TR/TE = 4.0/2.0 ms) and 18.4 s for the FLASH experiment (TR/TE = 4.5/2.0 ms). Table 1 summarizes the SNR efficiency of the TrueFISP experiment compared to the FLASH experiment for four different regions.

TrueFISP sequence, because the T2-to-T1 ratio, which determines the signal in TrueFISP, should be constant for different Gd-DTPA concentrations.

Fig. 3 shows a comparison between a TrueFISP, a FLASH and a spin echo image of a sunflower with a resolution of 78 μm × 78 μm × 500 μm. The TrueFISP image shows high signal in the surrounding water (ROI1) and in the homogeneous plant tissue (ROI2). However, a significant signal loss in the inhomogeneous part of the plant tissue (ROI3) can be detected. The total acquisition time, the SNR of the three different regions and the efficiency of the different imaging sequences are summarized in Table 2. Fig. 4 compares a TrueFISP image of a section of a formalin-fixed human heart with a FLASH image. The images show the same spatial resolution, however the SNR efficiency is increased by a factor of 2.2 in myocardial tissue for the TrueFISP sequence. Fig. 5 shows a magnification of a segmented TrueFISP image of a beating isolated rat heart compared with a FLASH image. The in-plane resolution is 78 μm with a slice thickness of 500 μm. In order to obtain nearly the same image contrast in the myocardium, a TE = 19.0 ms was chosen for the FLASH image. The total acquisition time was 51 s for the TrueFISP image and 14 min for the FLASH image. The SNR in myocardium is nearly the same in both images, whereas the TrueFISP image shows a 20% higher SNR in the balloon. The TrueFISP image shows additionally the well-known high vessel contrast.

4. Discussion

The present study demonstrates the range of applications of TrueFISP for microscopic experiments at high fields. If macroscopic field inhomogeneities can be avoided due to an optimized shimming procedure, artifact-free TrueFISP images can be obtained at high static magnetic field strengths. For all experiments shown here, a linewidth less than 45 Hz was obtained. This means that the range of frequencies across the image plane is within the plateau of the intensity profile of the transverse magnetization (Fig. 1) and thus banding artifacts could be avoided. The achievable sig-

Table 1
SNR efficiency (η) of TrueFISP compared with FLASH for a phantom doped with different concentrations of Gd-DTPA

	H_2O	H_2O + 0.25 mM Gd-DTPA	H_2O + 0.5 mM Gd-DTPA	H_2O + 1.0 mM Gd-DTPA
$\eta_{TrueFISP}/\eta_{FLASH}$	4.9	2.0	1.4	1.1

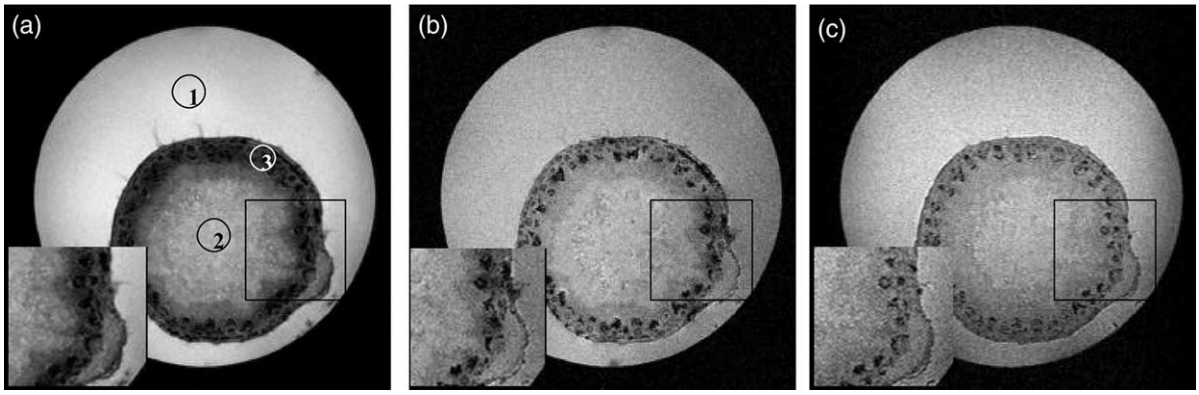

Fig. 3. TrueFISP (a), FLASH (b), and spin echo (c) image of a sunflower with a resolution of 78 μm × 78 μm × 500 μm. Table 2 compares the total acquisition time, the SNR and the efficiency of the different imaging techniques. ROI1, surrounding water; ROI2, homogenous plant tissue; ROI3, inhomogeneous plant tissue.

Table 2
Comparison of total acquisition time, SNR and efficiency (η) of TrueFISP, FLASH and spin echo experiments (ROI1, surrounding water; ROI2, homogeneous plant tissue; ROI3, inhomogeneous plant tissue)

	TrueFISP	FLASH	Spin echo
T_{ACQ}	16.4 s	41.0 s	1 h
SNR [ROI1]	46.6	17.8	21.5
η [ROI1]	89.1	21.5	2.8
SNR [ROI2]	39.8	18.0	20.9
η [ROI2]	76.1	21.8	2.7
SNR [ROI3]	7.4	12.4	15.7
η [ROI3]	14.2	15.0	2.0

nal and accordingly the achievable SNR in TrueFISP experiments depends mainly on the T2-to-T1 ratio. For example, the vessels in Fig. 5 have a high T2-to-T1 ratio, which results in a high signal compared to the signal obtained from the heart tissue.

However the image contrast of TrueFISP is not exclusively characterized by T2-to-T1 ratio. It is also influenced by the sensitivity of TrueFISP to susceptibility differences and can be modified with sequence repetition time. A longer TR means a longer dephasing period and thus, the image contrast can be made to be similar to the contrast in the gradient echo images. For example, the TrueFISP image of the isolated rat heart (Fig. 5) shows a similar contrast behavior to the corresponding gradient echo image. The orientation of myocardial fibers is visible in both images. The main difference of these two images is the well-known high vessel contrast of the TrueFISP sequence.

As mentioned before, the contrast in TrueFISP images can be modified by using different repetition times or applying different phase cycles of the radiofrequency pulse [11–13]. This could potentially be used to introduce a novel tissue contrast in microscopic experiments. Figs. 4b and c show the difference in image contrast between a TrueFISP image with alternating RF phases

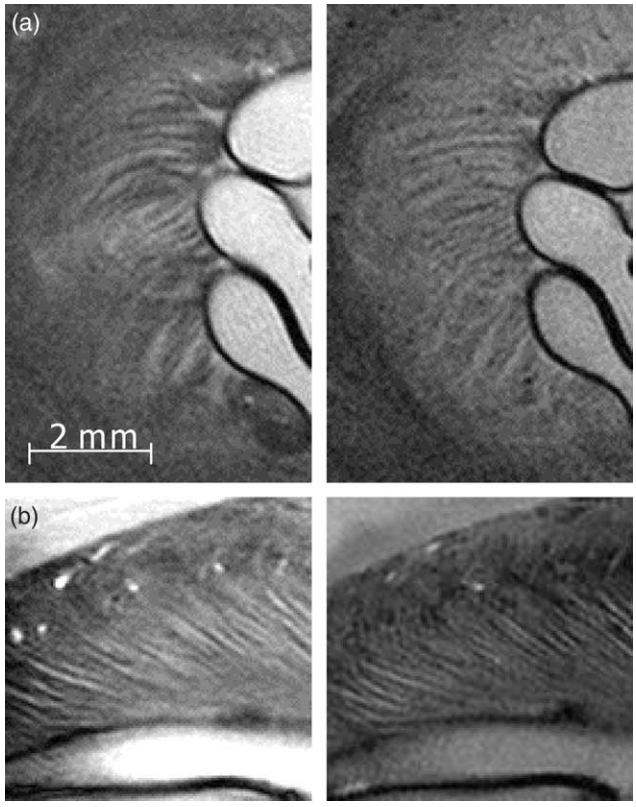

Fig. 5. Magnification of a TrueFISP image (left) and FLASH image (right) of a beating isolated rat heart in the short axis view (a) and (b) in the long axis view with an in-plane resolution of 78 μm and a slice thickness of 500 μm. Total acquisition time was 51 s for the TrueFISP and 14 min for the FLASH experiment.

(b) and an image with the same RF phase (c). The sequence with alternating RF phases shows a flat profile for off-resonance frequencies near 0, whereas the sequence with the same RF phase shows a flat profile for off-resonance frequencies near π. Thereby, the off-resonance bandwidth is shifted and the sensitivity of TrueFISP to a certain bandwidth of frequencies is modified

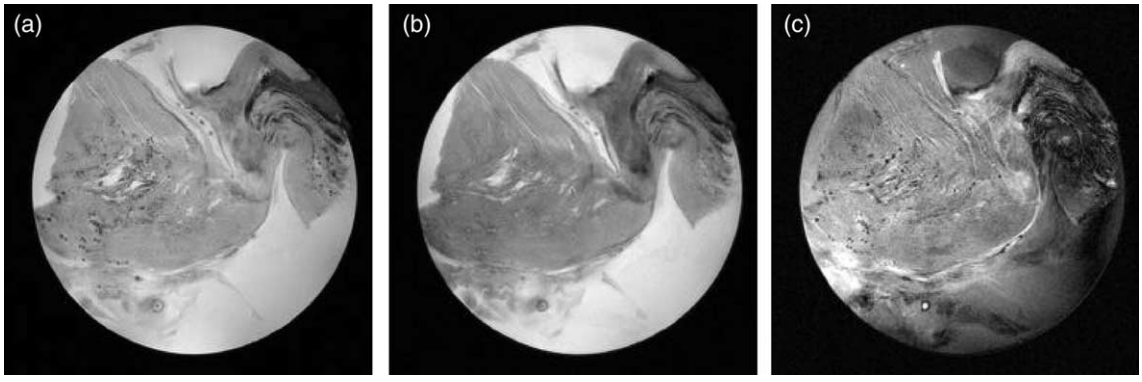

Fig. 4. Comparison of a FLASH image (a), a TrueFISP image with alternating RF phases (b), and with a constant RF phase (c) of a part of a formalin-fixed human heart with a resolution of 78 μm × 78 μm × 500 μm. In this example, the SNR efficiency of the TrueFISP image (b) is increased by a factor of 2.2 in comparison to the FLASH image (a).

which results in different image contrast as demonstrated in Figs. 4b and c. Using this modification of RF phase cycling, a detailed insight into the myocardial microstructure is obtained.

The TrueFISP sequence was tested on typical fields of applications of microscopic experiments and in all examples a SNR gain of the TrueFISP sequence was obtained when compared to conventional gradient echo and spin echo experiments. For the plant experiment, the SNR efficiency is increased by a factor of 3.5 for plant tissue (ROI2) and by a factor of 4.1 for the surrounding water (ROI1) when compared to gradient echo images (Table 2). In comparison to spin echo images, the SNR efficiency of TrueFISP shows an increase of 28.9 for plant tissue (ROI2) and 32.3 for the surrounding water (ROI1). Due to the high SNR of TrueFISP compared to conventional gradient echo and spin echo sequences, TrueFISP could allow faster microscopic experiments.

The TrueFISP acquisition proved successful and useful in providing the spatial, temporal, and contrast resolution for various microscopic experiments. However, it could not be concluded that TrueFISP is always superior to conventional gradient echo and spin echo techniques at high fields. With extremely inhomogeneous objects, for example the air–tissue interface inside animals or samples with large susceptibility differences, it could be difficult to achieve a sufficient linewidth at high fields in order to avoid the banding artifacts of the TrueFISP sequence. In addition, signal loss due to the sensitivity to tissue specific microscopic field inhomogeneities could reduce the SNR gain of TrueFISP. For the inhomogeneous plant tissue (ROI3) the TrueFISP experiment shows a loss of SNR efficiency compared to the gradient echo experiment (Fig. 3/Table 2). Further experiments on the sensitivity to tissue specific microscopic field inhomogeneities are currently underway in our laboratory. In comparison to conventional imaging techniques, the SNR gain of TrueFISP is obvious. However it must be taken into account that a SNR comparison is always difficult and is strongly influenced by the chosen acquisition parameters such as TE, TR, and flip angle and that these parameters could only be optimized for one selective tissue and not for the whole object. For microscopic experiments, the achievable SNR is not the only important parameter. A contrast-to-noise ratio (CNR) is also essential. Whether TrueFISP could provide always the desired contrast depends on the particular application and must be investigated in further experiments. For very inhomogeneous objects, such as plants, conventional gradient echo or spin echo experiments could be superior to TrueFISP experiments. However, the CNR of structures with a high T2-to-T1 ratio, for example the vessels in the isolated heart, is much better in TrueFISP images as in gradient echo and spin echo images.

5. Conclusion

We have demonstrated that TrueFISP sequences, once believed to have limited application in imaging at high fields due to the sensitivity to susceptibility differences, can provide good contrast, spatial and temporal resolution for microscopic experiments. The high SNR efficiency of TrueFISP compared to conventional gradient and spin echo techniques allows faster acquisition times and/or an improvement in spatial resolution for microscopic experiments. Since the resolution in NMR microscopy is ultimately limited by the SNR available per unit time, refocused steady-state sequences such as TrueFISP could become a powerful tool for microscopic experiments at high fields.

Acknowledgments

This work was supported by Grant SFB 355 and Graduiertenkolleg "Magnetische Kernresonanz in vivo und in vitro," Deutsche Forschungsgemeinschaft.

References

[1] A. Oppelt, R. Graumann, H. Barfuß, H. Fischer, W. Hartl, W. Schajor, FISP—a new fast MRI sequence, Electromedica 54 (1986) 15–18.
[2] V.S. Deshpande, S.M. Shea, Y.C. Chung, R.M. McCarthy, J.P. Finn, D. Li, Breath-hold three-dimensional True-FISP imaging of coronary arteries using asymmetric sampling, J. Magn. Reson. Imag. 15 (2002) 473–478.
[3] K. Scheffler, J. Hennig, T_1 quantification with inversion recovery TrueFISP, Magn. Reson. Med. 45 (2001) 720–723.
[4] W.R. Overall, S.M. Conolly, D.G. Nishimura, B.S. Hu, Oscillating dual-equilibrium steady-state angiography, Magn. Reson. Med. 47 (2002) 513–522.
[5] R. Merrifield, J. Keegan, D. Firmin, G.Z. Yang, Dual contrast TrueFISP imaging for left ventricular segmentation, Magn. Reson. Med. 46 (2001) 939–945.
[6] V.S. Deshpande, S.M. Shea, G. Laub, O.P. Simonetti, J.P. Finn, D. Li, 3D magnetization-prepared True-FISP: a new technique for imaging coronary arteries, Magn. Reson. Med. 46 (2001) 494–502.
[7] M. Haacke, R.W. Brown, M.R. Thompson, R. Venkatesan, in: Magnetic Resonance Imaging, Wiley-Liss, New York, 1999, p. 480.
[8] K. Scheffler, O. Heid, J. Hennig, Magnetization preparation during the steady state: fat-satured 3D TrueFISP, Magn. Reson. Med. 45 (2001) 1075–1080.
[9] Y. Zur, S. Stokar, P. Bendel, An analysis of fast imaging sequences with steady-state transverse magnetization refocusing, Magn. Reson. Med. 6 (1988) 175–193.
[10] K. Scheffler, E. Seifritz, D. Bilecen, R. Venkatesan, J. Hennig, M. Deimling, M. Haacke, Detection of BOLD changes by means of a frequency-sensitive trueFISP technique: preliminary results, NMR Biomed. 14 (2001) 490–496.
[11] S.S. Vasanawala, J.M. Pauly, D.G. Nishimura, Fluctuating equilibrium MRI, Magn. Reson. Med. 42 (1999) 876–883.
[12] S.S. Vasanawala, J.M. Pauly, D.G. Nishimura, Linear combination steady-state free precession MRI, Magn. Reson. Med. 43 (2000) 82–90.
[13] E.M. Haacke, P.A. Wielopolski, J.A. Tkach, M.T. Modic, Steady-state free precession imaging in the presence of motion: applica-

tion for improved visualization of the cerebrospinal fluid, Radiology 175 (1990) 545–552.
[14] J.L. Duerk, J.S. Lewin, M. Wendt, C. Petersilge, Remember true FISP? A high SNR, near 1-second imaging method for T2-like contrast in interventional MRI at .2 T, J. Magn. Reson. Imag. 8 (1998) 203–208.
[15] M. Deimling, O. Heid, Magnetization prepared true FISP imaging, in: Proceedings of the 2nd Annual Meeting of the Society of Magnetic Resonance, San Francisco, 1994, p. 495.
[16] J. Bundy, O. Simonetti, G. Laub, J.P. Finn, Segmented TrueFISP cine imaging of the heart, in: Proc. 7th ISMRM Scientific Meeting, Philadelphia, 1999, p. 1282.
[17] M.J. Firbank, A. Coulthard, R.M. Harrison, E.D. Williams, A comparison of two methods for measuring the signal to noise ratio on MR images, Phys. Med. Biol. 44 (1999) N261–N264.